Metallurgy and materials
*Metalurgia e materiais*

# Obtainment of a new metal matrix composite from the recycling of UNS S31803 duplex stainless steel by powder metallurgy

http://dx.doi.org/10.1590/0370-44672021750077

**Lucas Rafael da Silveira**[1,2]
https://orcid.org/0000-0002-8443-5612
**Marcela Silva Lamoglia**[1,3]
https://orcid.org/0000-0001-9768-4581
**Pedro Henrique Gonçalves**[1,4]
https://orcid.org/0000-0001-9060-5959
**Bruna Horta Bastos Kuffner**[1,5]
https://orcid.org/0000-0003-3306-5102
**Gilbert Silva**[1,6]
https://orcid.org/0000-0002-6636-4013

[1]Universidade Federal de Itajubá - UNIFEI,
Instituto de Engenharia Mecânica,
Itajubá – Minas Gerais - Brasil.

E-mails: [2]lucasrafael09@yahoo.com.br,
[3]marcelalamoglia@unifei.edu.br,
[4]pedrogoncalves@unifei.edu.br,
[5]brunakuffner@hotmail.com, [6]gilbert@unifei.edu.br

## Abstract

The purpose of circular economy is to maximize resources efficiency. With the increase in consumption of raw materials, energy and waste generation, recycling is necessary for environmental and industrial reasons. Thus, the powder metallurgy, together with mechanical milling, stands as a new method for scraps recycling. This study aimed to produce UNS S31803 duplex stainless steel powders, with vanadium carbide (VC) addition as reinforcement, through mechanical milling. Different uniaxial compaction pressures (700, 800 and 900 MPa) were used, as well as sintering temperatures (1200, 1240 and 1280 °C) and times (1, 1.5 and 2 hours), in order to determine the best conditions. Particle size analysis, scanning electron microscopy and x-ray diffraction were used to characterize the powders. It was observed that the use of VC increased the comminution during the milling process, being obtained an average particle size of 42 µm. The highest density obtained was of 82% and hardness of 72%, in comparison with the steel from the manufacturing process. According to the analysis, it was verified that this method is viable, becoming an alternative route to reuse UNS S31803 duplex stainless steel scraps.

**Keywords:** UNS S31803 Duplex Stainless Steel, Vanadium Carbide, Recycling, High Energy Ball Milling; Powder Metallurgy.

## 1. Introduction

Metal production is related to a generation of significant amount of wastes. In general, solid and liquid wastes from metallurgy contain fractions of rich elements, which are suitable for other metallurgies, such as raw materials. The objective of circular economy (CE) is to maximize resource efficiency (RE), increasing the life cycle of products and using wastes as byproducts. The CE model is an economic system that aims to reduce the wastes production, through the reuse and recycling of materials already available (Reuter *et al*., 2019).

CE not only reduces the volume of wastes, but also mitigates the depletion of non-renewable resources, due to economic development, with consequent environmental benefits in terms of energy savings during production processes. Additionally, because of the reduction of offer and subsequent need to reuse resources to obtain proper cost-efficiency relation, CE must be encouraged, publicized and disseminated. The development of a CE approach may conduce to the exploitation of new opportunities for urban and environmental protections. Besides, it improves long-term sustainability, contributing to resources preservation and lower costs for industries (Ozola *et al*., 2019).

The powder metallurgy (PM) is a technique with great potential to be used as a tool for CE. It happens because through the steps of powder obtainment, pressing and sintering, it is possible to create a new component from a material that reached the end of its life cycle. PM offers a wide range of possibilities, such as the production of workpieces with complex geometries, high melting points and differentiated chemical compositions. It is considered the only approach to reuse materials, beyond casting. Also, it is considered cleaner, since it does not produce wastes, such as scraps, and also, it emits smaller amounts of greenhouse gases in the atmosphere (Danninger *et al*., 2017).

One of the most effective methods of powder obtainment is the high energy ball milling (HEBM). This process involves energetic compressive forces over a powder mixture, that provokes cold welding under pressure and particles fracture. In this way, the synthesis of alloys on nanometric scale, metastable composites, amorphous materials, mechanical activation of chemical reactions and others, can occur (Suryanarayana, 2001).

Duplex stainless steels (DSSs) are constituted by volumetric fractions of ferrite and austenite, in proportions approximately equal, exhibiting mechanical properties and corrosion resistance superior to other stainless steels. However, they are materials that demand special needs at high operational temperatures. Thus, DSSs have been object of many studies, due to a diversity of fields where they can be used. Regarding their microstructure, stainless steels are basically classified in: ferritic, austenitic, martensitic, hardened by precipitation and duplex. The development of these steels occurred in the first decades of the 20th century, in the United Kingdom and Germany. Lately, superaustenitic or superduplex stainless steels were also developed (Gunn, 1997; Totten, 2006).

Stainless steels prepared by powder metallurgy have attracted the attention of researchers, due to the capacity of this route of producing components with complex shapes, good mechanical properties and superior corrosion resistance (Shashanka, 2014). Aguiar (2008) studied the behavior of UNS S32520 super duplex stainless steel scraps by HEBM. By the same way, Mendonça *et al.* (2018) used HEBM to mill UNS S31803 duplex stainless steel scraps, and observed that the best milling condition was with addition of vanadium carbide during the process. Also, the work of Yonekubo (2009) presented a microstructural characterization of UNS S32520 super duplex stainless steel (UR 52N*) processed by HEBM.

In order to improve the mechanical properties of steels produced by powder metallurgy, metal-ceramic composites were created, in which the addition of carbides as reinforcement are used. These materials present great properties, such as high melting point (around 4000 °C), high hardness and good electrical and thermal conductivity. Also, when added to the high energy ball milling process, carbides have the ability to improve the milling of metallic materials (Trueman *et al.*, 1999; Gubernat & Zych, 2014; Suryanarayana, 2001).

The addition of ceramic carbides in the HEBM aims to accelerate the reduction of particles size, as carbides are very stable constituents, with high hardness. When combined with stainless steel scraps, that have ductile behavior, a ductile-brittle alloying system is created. During HEBM, the collision between the milling agents (scraps + carbides + spheres) are responsible for generating a region of generalized stresses in the ductile particle (scraps), leading to rupture in a shorter processing time. Therefore, the addition of vanadium carbide (VC) in the powder metallurgy route was intended to reduce processing time, in addition to being a barrier to grain growth during heat treatments, where it is possible to increase the mechanical strength by grain size refining (Suryanarayana, 2001; Barbedo *et al.*, 2021; Huang *et al.*, 2018).

In this research, UNS S31803 duplex stainless steel scraps with addition of VC, were processed by the powder metallurgy route. The intention was to develop a new metal-ceramic composite, and also, remove this waste from the environment. The main advantages of submitting this steel by this technique are the possibility to combine it with carbides, increasing then its milling efficiency and mechanical strength.

## 2. Materials and methods

The materials used in this research were UNS S31803 duplex stainless steel laminated plate, with 5mm of thickness, produced by the company Aperam® South America, with density of 7.80 g/cm³, and vanadium carbide from the company Hermann C. Stark®, with granulometry of 3 to 4 µm and density of 5.71 g/cm³. Table 1 shows the chemical composition values for the UNS S31803 duplex stainless steel, provided by the manufacturer.

Table 1 – Chemical composition of UNS S31803 duplex stainless steel (% by weight).

| Chemical composition by element (wt%) | | | | | | | | | | | |
|---|---|---|---|---|---|---|---|---|---|---|---|
| **Fe** | **C** | **Cr** | **Mn** | **Ni** | **Mo** | **Si** | **Co** | **Cu** | **N** | **Nb** | **V** |
| 66.500 | 0.018 | 22.220 | 1.480 | 5.590 | 3.080 | 0.450 | 0.130 | 0.280 | 0.180 | - | - |

The scraps of UNS S31803 steel were obtained through machining, at low rotational speed (≈ 40 rpm), and without use of lubrication, to avoid contamination. In the high energy ball milling (HEBM) process, UNS S31803 duplex stainless steel scraps and 3% of vanadium carbide (VC) were separated. Posteriorly, these materials were inserted into a stainless steel jar, with 200 g of capacity, together with milling spheres of AISI 52100 steel, with different diameters: 6.00 mm, 12.00 mm and 18.00. The milling jars were closed and immediately, argon gas was introduced inside, in order to prevent oxidation during HEBM. A planetary ball mill Noah-Nuoya® NQM 0.2 L was used in the HEBM, and the milling parameters followed according to Table 2.

Table 2 – Parameters used in the HEBM process of UNS S31803 duplex stainless steel .

| Milling parameter | Value |
|---|---|
| Speed | 350 rpm |
| Ball to powder ratio | 20:1 |
| Time | 100 hours |
| Downtime | 15 minutes/hour |
| Shielding gas | Argon |

The choice of using 3% of VC in the miling of UNS S31803 stainless steel scraps was based on the study by Mendonça *et al*. (2018), as they investigated the behavior of the addition of VC with proportions of 0, 1 and 3% by weight in this same steel by HEBM. Through particle size analysis, they observed that the percentage of 3% was the most effective, as it can be seen in Table 3, since it obtained the smallest particle size among all compositions.

Table 3 – Particles size of the UNS S31803 stainless steel scraps with different VC additions (Mendonça *et al.*, 2018).

| Milling time | 0% VC | 1% VC | 3% VC |
|---|---|---|---|
| 10 h | 150 - 450 µm | 100 - 400 µm | 40 - 200 µm |
| 50 h | 100 - 250 µm | 50 - 200 µm | 20 - 170 µm |

The UNS S31803 duplex stainless steel milled with 3% of VC was selected with granulometry below 300 µm (50 mesh), with the use of a strainer disturber. The objective was to separate rough particles, which were classified as waste, and later discarded. After this, a tension relief thermal treatment was performed in the powders, inside a quartz tube at 1050 °C for 30 minutes, under vacuum, with a negative pressure of $10^{-2}$ mbar and later, cooled down in water (at room temperature). The powder compaction was executed in a uniaxial press Schulz®, using a matrix with 8 mm of diameter. The compaction pressure was applied during 30 seconds, being this procedure repeated 3 times. After pressing, the samples were sintered in a Nabertherm® model HT04/17 furnace, with a heating rate of 5 °C/minute. The conditions used in the compaction and sintering can be seen in Table 4. These different conditions were performed to determine the best powder metallurgy parameters for the UNS S31803 duplex stainless steel powder with 3% of VC. The values mentioned in Table 2 for compaction pressure and sintering temperatures and times were based on the studies of Mendonça *et al*. (2018), Tański *et al*. (2014) and Garcia *et al*. (2012).

Table 4 – Parameters used in the compaction and sintering processes of the UNS S31803 duplex stainless steel powder with 3% of VC.

| Conditions | Compaction pressure (MPa) | Sintering Temperature (°C) | Sintering Time (hours) |
|---|---|---|---|
| Condition 1 | 700 | 1200 | 1.0 |
| Condition 2 | 800 | 1240 | 1.5 |
| Condition 3 | 900 | 1280 | 2.0 |

The powders and sintered samples obtained were microstructurally and mechanically characterized. The average particles size and distribution were obtained using a Microtrac® laser granulometer. A scanning electron microscope Carl Zeiss® Evo MA 15 was applied, in the modes secondary electron (SE), backscatter electron detector (BSD) and energy dispersive spectroscopy (EDS) as punctual analysis and mapping, in order to identify the variation, morphology and chemical composition of the powders, besides the sintered microstructure. Sintered samples porosity and diffusion analyzes were obtained with the assistance of an optical microscope Olympus® BX41M. The identification of the phases present in the UNS S31803 duplex stainless steel was performed in the material as received (bulk), as powder with 3% of VC milled for 50 hours without stress relief thermal treatment and after sintering for condition 3 (the most severe condition). It was performed using an x-ray diffractometer Panalytical® X'Pert PRO. A chrome tube was selected, with CrKα having λ = 2.28976 Å of radiation, sweep from 65 to 130° and step of 0.04° for 2 seconds. For the compression strength test, an EMIC® DL universal testing machine was employed. The samples for this test were manufactured with 12.00 mm of height and 8.00 mm of diameter. These dimensions were defined in order to obtain an H/D ratio of 1.5, as stipulated in the ASTM E09 (2019) standard. With the stress-strain curves, it was possible to determine the elastic modulus of the sintered samples. The analysis of elastic modulus was chosen because this property is related to atomic and non-microstructural bonds. Ultimately, hardness measurements were executed in an Otto Wolpert-Werke® Testor HT durometer, with Rockwell B (HRB) scale, according to the ISO 4498 (2005) standard. A preload of 10 kgf and a final load of 100 kgf were applied. Comparisons were also performed between the mechanical properties of the casted and PM processed UNS S31803 steel, with the intention to determine the effectiveness of the PM route, since that the authors desired to obtain a material with characteristics similar to the casted material.

## 3. Results and discussion

### 3.1 Granulometric distribution analysis

Figure 1 shows the granulometric distribution curve of the UNS S31803 duplex stainless steel powder with 3% of VC after HEBM. It was possible to identify an average particles size of 42 µm. Observing the particle distribution, a crescent asymmetric bimodal distribution is noted. According to the results, the larger part of the powder population has sizes between 44 and 53 µm. The minimum and maximum particle sizes found were between 7 and 209 µm, respectively.

The distribution is relatively large, which can be considered a good characteristic, because during the compacting

process, smaller particles spread among the bigger ones, resulting in a higher green density, and also, more contact points between particles, easing neck formation during sintering. The horizontal axis in Figure 1 indicates the particles size, while the vertical axis corresponds to percentage (blue) and accumulated (green) particles. The D value parameters generated by the test are shown in Table 5. It is important to highlight that the D values obtained indicate that the percentages of particles of 10, 50 and 95%, respectively, have sizes equal or inferior to those presented in Table 5.

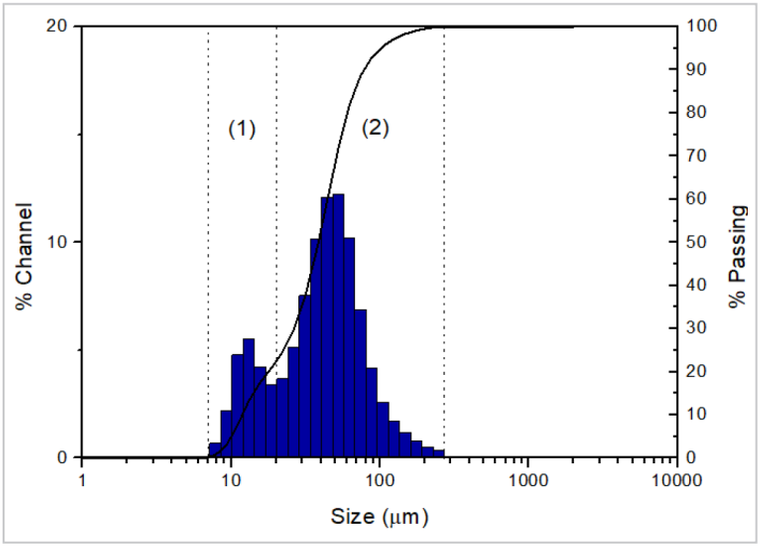


Figure 1 – Granulometric distribution curve of the UNS S31803 duplex stainless steel powder with 3% of VC after HEBM.

Table 5 – Particles size distribution of the UNS S31803 duplex stainless steel powder with 3% of VC after HEBM.

| D values | Size (μm) |
|---|---|
| D10 | 11.29 |
| D50 | 37.76 |
| D95 | 94.87 |

It is highlighted that the VC particles inserted in the milling process present sizes between 3 and 4 μm, and the granulometric analysis did not show particles in this range size. It indicates the great homogeneity between the particles of this carbide and the steel after HEBM, which occurs as a consequence of the ductile-brittle alloying system. What happens in this condition is that the VC particles accommodate themselves in the interlamellar spaces of the UNS S31803 duplex stainless steel scraps during milling, forming a single particle after the comminution process (Suryanarayana, 2001). Comparing the values found in Table 4 with those obtained by Mendonça *et al.* (2018), it is noted that both are similar, since that the authors found in the HEBM process of the UNS S31803 duplex stainless steel milled with VC a decrease in the average particles size of 8% (from 46 μm to 42 μm).

## 3.2 Green density, sintered density and porosity analysis

According to Table 2, the sintering conditions used were different, and consequently, they influenced the solid diffusion process. Figure 2 shows the optical micrographs of the UNS S31803 duplex stainless steel with 3% of VC after sintering, for conditions 1, 2 and 3. Observing Figure 2a for condition 1, it is noted that diffusion was slow, pointed out by the first stage of sintering, shown by only few neck formations. The neck is characterized by the gradual elimination of the grain boundaries between two or more particles that were initially in contact, forming then a single particle at the end of the diffusional process (neck completely formed or full third stage of sintering) (Dzepina *et al.*, 2019). In condition 2 (Figure 2b), the diffusion process was more advanced, in which the increasing of necks is observed, characterized by the intermediary stage of sintering. Finally, condition 3 (Figure 2c) achieved the intermediary and final stages of sintering, where the diffusional process was more pronounced, when compared to conditions 1 and 2. A good consolidation between particles, by rounding and elimination of remaining pores, was verified.

The justifications for better diffusion found in condition 2 and even better in condition 3 are due to the higher compacting pressure and sintering time and temperature used, when compared to condition 1. In condition 3, the particles were more accommodated after compaction than in conditions 1 and 2, as a consequence of the higher pressure applied during uniaxial pressing, which implies in higher atomic diffusion energy, and consequently, better densification after heat treatment. In terms of powder metallurgy, the densification is defined as the reduction or elimination of the pores inside of the material microstructure after sintering, which were produced during the compaction process of the forerunner powders (German, 2005; Dias *et al.*, 2019).

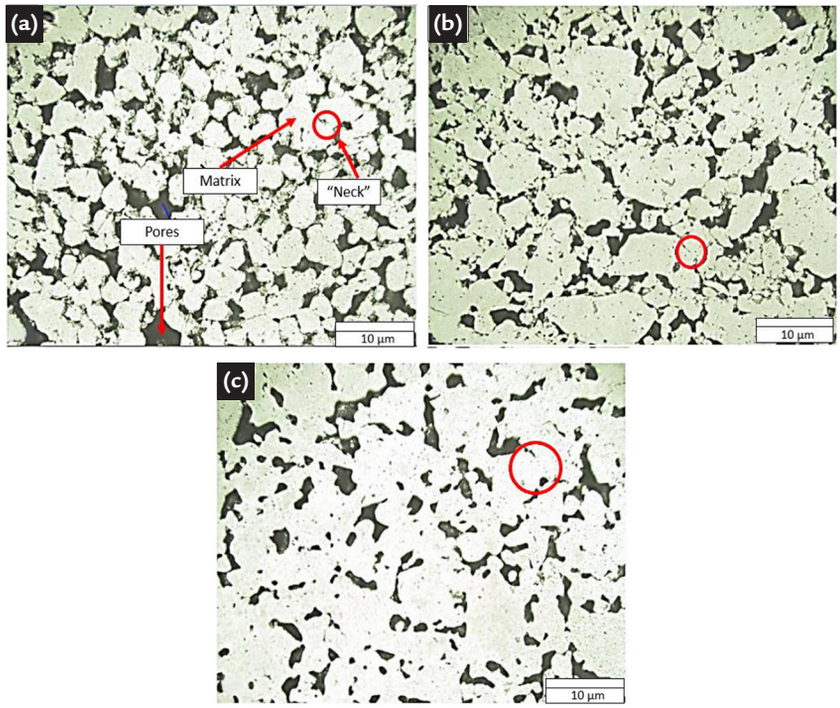


Figure 2 – Optical micrographs of the UNS S31803 duplex stainless steel with 3% of VC after sintering, for conditions (a) 1 (b) 2 and (c) 3 (Table 3).

In order to analyze the densification efficiency of the UNS S31803 duplex stainless steel with 3% of VC addition, the density of the samples before sintering (green density), as well as the density and porosity after sintering were analyzed (Table 6). From the green to sintered density, the 3 conditions presented gain in densification. This is represented by the increase in the density values and decrease in porosity, due to the atomic diffusion.

In terms of green density, it can be seen that from condition 1 to 2, there was an increase of 1.87% in green density. From condition 2 to 3, there was practically no difference, while for the sintered density, there was noted an increase of 3.23% in the density from condition 1 to 2. From condition 2 to 3, an increase of 2.37% was observed. It reveals an average pattern of 2.4 – 3.4% of increase from one condition to the next. In general, from condition 1 to 3, there was observed an increase of 5.52% in the densification of the samples. Also, comparing the sintered densities with the density of UNS S31803 duplex stainless steel as casted (7.80 g/cm³), condition 1 presented 76.80% of the casted density, condition 2 presented 79.36% and condition 3, 81.28%. Since the powder metallurgy is a technique that induces a high percentage of pores in the material microstructure, a smaller density is expected, when compared to the casted material (with practically no presence of pores).

Lastly, comparing the green density with the sintered density, it can be seen that after sintering, condition 1 gained 3.84% of densification. For condition 2, a densification gain of 5.17% was observed. For condition 3, a gain of 7.57% was verified. The greater gain from condition 1 to 2 and from condition 2 to 3 was expected, since according to Table 3, these conditions are related with higher compaction pressures and sintering temperatures and times.

Table 6 – Green density, sintered density and porosity values for UNS S31803 duplex stainless steel with 3% of VC addition.

| Conditions | Green density (g/cm³) | Sintered density (g/cm³) | Porosity (%) |
|---|---|---|---|
| Condition 1 | 5.76 | 5.99 | 33.08 ± 2.85 |
| Condition 2 | 5.87 | 6.19 | 25.69 ± 2.18 |
| Condition 3 | 5.86 | 6.34 | 18.25 ± 1.09 |

The porosity was evaluated by the values indicated in Table 6 and by the micrographs of Figure 3. According to Table 6, from condition 1 to 2, the porosity decreased 22.34%, and from condition 2 to 3, there was a decrease of 28.92%. In general, from condition 1 to 3, there was a decrease of 44.83% in porosity. Already Figure 3 shows the porosity micrographs for conditions 1 and 3 (the most extremes). The highlighted red areas correspond to the sintered matrix, while the green areas, to the pores. As it can be seen, condition 1 (Figure 3a) presents higher porosity volume than condition 3 (Figure 3b).

Comparing the results obtained for porosity with the values of density, it is possible to observe that both are directly connected. The higher the density of the material after sintering, the lower its porosity. It occurs because the higher density is a consequence of the reduction in the volume of pores inside of the material, due to greater atomic diffusion. As noted, condition 3 obtained the smallest porosity, because of the more severe conditions of compaction and sintering that was submitted. Higher compacting loads reflect in more contact between particles, while elevated sintering temperatures offer more energy for atomic diffusion and neck formation.

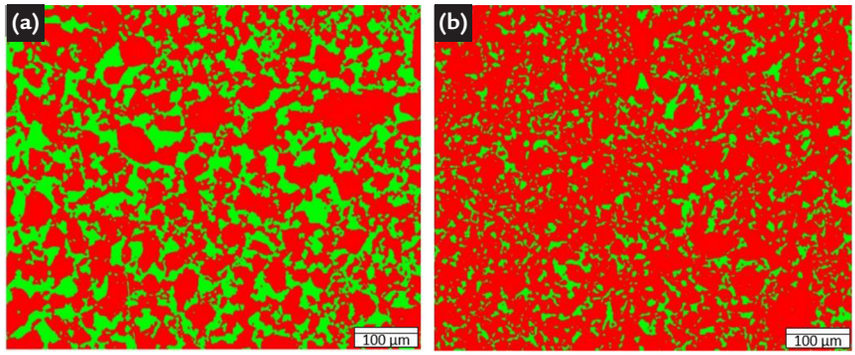


Figure 3 – Porosity analysis of the sintered UNS S31803 duplex stainless steel with 3% of VC for conditions (a) 1 and (b) 3 (Table 3).

In parallel to the optical microscopy analysis, a scanning electron microscopy (SEM) test was performed, in BSD and EDS modes, specifically in the mapping mode, aiming to identify the location of the VC ceramic particles added during HEBM (Figure 4). The chemical elements Fe, Cr, C, Mo, Mn, Ni and Si belong to the chemical composition of UNS S31803 duplex stainless steel (Figure 4a). The V element corresponds to the vanadium carbide inserted during the HEBM (Figure 4b). It can be noted that the V particles are homogeneously distributed in the steel matrix, revealing that the milling process was effective. This consequently implies in better mechanical properties for this material. The Al element is not present in the initial chemical composition of the UNS S31803 duplex stainless steel, being its presence from the metallographic process, since the polishing solution used is composed by alumina ($Al_2O_3$).

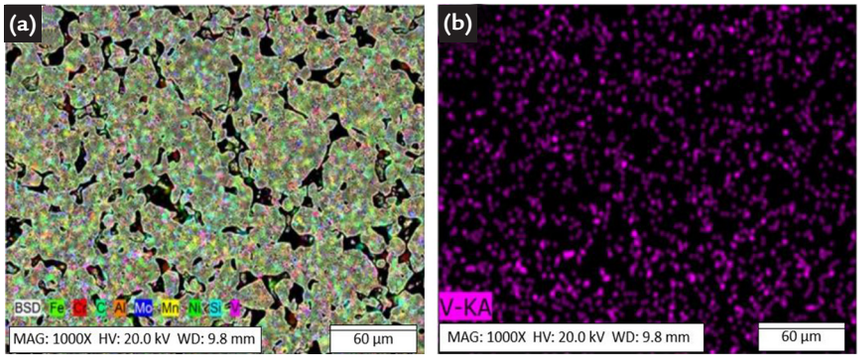


Figure 4 – SEM/EDS/Mapping analysis of the UNS S31803 duplex stainless steel with 3% of VC (a) Steel main chemical elements (b) VC particles dispersion (Table 3).

### 3.3 X-ray Diffraction test

The material as received for this study must have the microstructure of a duplex stainless steel, composed by austenite and ferrite (Figure 5). In the HEBM process, the material suffers reductions in particle size and minimal deformations in its crystalline structure. These deformations are represented in the x-ray diffraction analysis by the peak enlargement and intensity decrease. In the compaction processes, it is necessary that the powder used presents certain ductility, in order to obtain a green sample with higher quality. This will only happen if the crystalline structure of the material is preserved or recovered after the powder obtainment. For this, the material after conformation must be analyzed by x-ray diffraction, and its peaks must be as similar as possible to the material as received.

Figure 5 shows the x-ray diffractogram of the UNS S31803 duplex stainless steel as received, milled for 50 hours without stress relief thermal treatment and sintered at condition 3. It is observed that for the material after milling, the peaks presented enlargement and low intensity, when compared to the material as received, due to intense plastic deformation. It causes the amorphization of the crystalline lattice during the high energy ball milling process. It can also be seen in the diffractogram of Figure 5 that, after the milling process, there was a decrease in intensity and enlargement of the peaks of the ferrite (110) and austenite (111) phases. It is also possible to observe the disappearance of (200), (200), (311) and (222) austenite phase peaks and the relative peak intensity of ferrite (220).

The diffractogram of Figure 6 shows, in the regions of angles between 65° and 70°, that after the milling process, there was a decrease in intensity and enlargement of the ferrite (110) and austenite (111) peaks, compared to the material as received. It occurs due to non-uniform plastic deformations (microstrains) of the crystalline lattice, resultant from stacking failures, among other crystalline defects from the milling and particle size reduction process. After heat treatment, there is a decrease in the peaks width and an increase in their intensity. For the austenite phase, a significant increase in intensity was observed, since its crystallization occurred faster when compared to ferrite. This behavior is associated with the reduction of microstrains, caused by annealing, due to recovery and recrystallization processes (Suryanarayana, 2001).

After heat treatments of stress relief and sintering, the ferrite and austenite phases were observed. Figure 6 shows a peak displacement to the right, for the ferrite phase (110) at 68.382° after stress relief treatment and a 0.16° displacement after sintering for conditions 1, 2 and 3. For the austenite phase (111), a displacement of

0.20° after stress relief treatment was observed, as well as a displacement of 0.308° after sintering for conditions 1, 2 and 3. It characterizes the displacement of the crystallographic planes and changes in lattice parameter of the material after sintering.

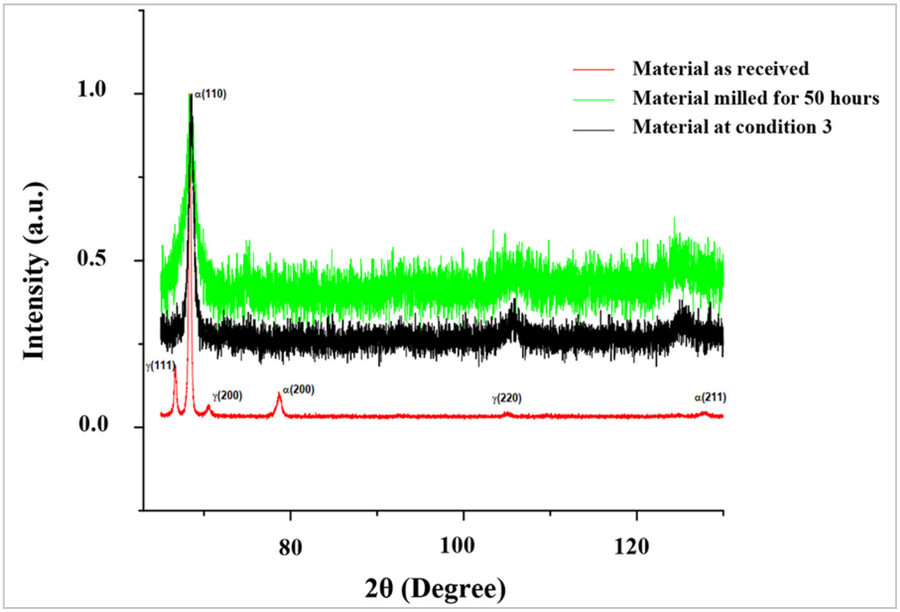


Figure 5 – Diffractogram of the UNS S31803 duplex stainless steel as received, milled for 50 hours and at condition 3 (Table 3).

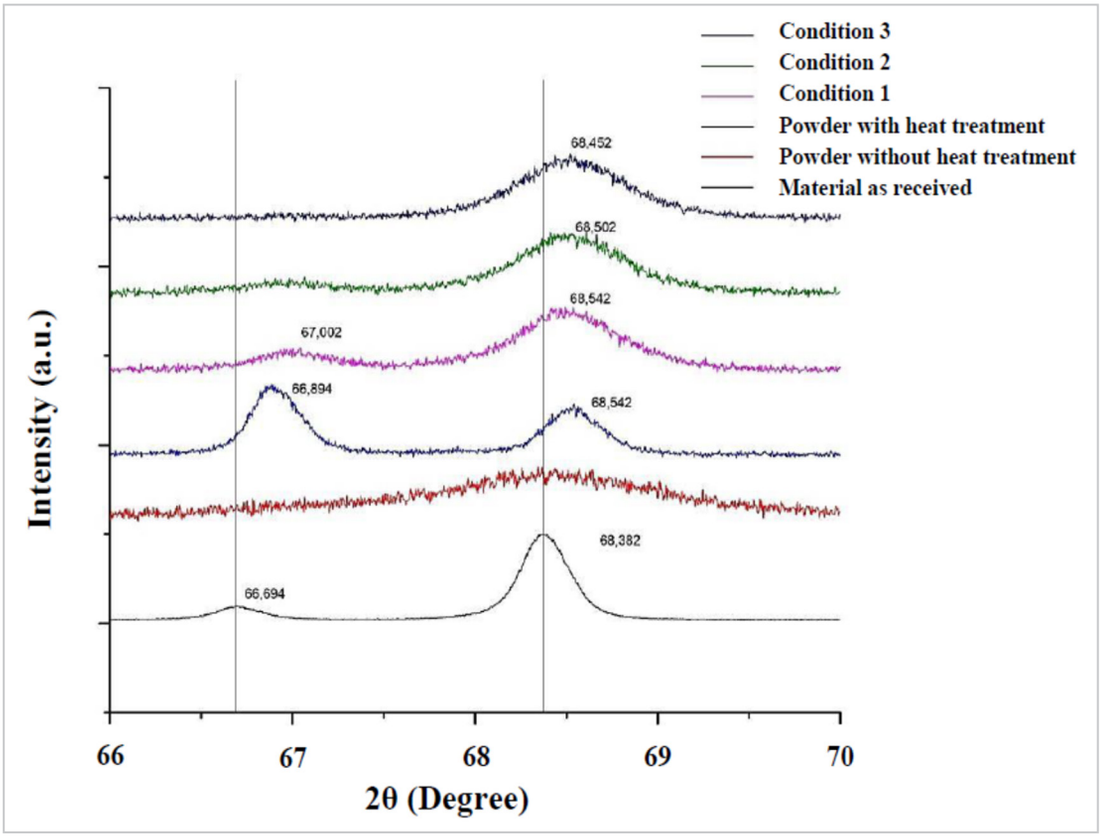


Figure 6 – Diffractogram of the UNS S31803 duplex stainless steel between 65° and 70° as received, milled for 50 hours with and without stress relief heat treatment and after sintering at conditions 1, 2 and 3 (Table 3).

### 3.4 Compressive strength test

Figure 7 shows the stress-strain curves of the sintered UNS S31803 duplex stainless steel with 3% of VC for conditions 1 (Figure 7a) and 3 (Figure 7b). Using these curves, it was possible to obtain the values of elastic modulus for each one of the analyzed samples (Table 7).

It is observed that the samples of condition 1, which presented worse densification and, consequently, higher porosity than the samples of condition 3 (porosity 44.8% higher than condition 3), obtained elastic modulus of 1.32 GPa, while the samples of condition 3, elastic modulus of 0.98 GPa. It represents an increase of 25.38% in the elastic modulus of the samples from condition 1 to condition 3.

Comparing these values with the elastic modulus of duplex stainless steel after casting of 200 GPa (Davis, 1994), it is verified that the samples produced

by PM presented significantly lower values, due to the higher percentage of porosity in their microstructure. It is well known in literature that the higher the pore percentage in a material, the lower its mechanical strength will be. It occurs as a consequence of some factors, such as: gross section loss, which locally reduces the effective stiffness of the steel, and stress concentrations near the pores, which lead to localized plastic deformations and development of microcracks and consequently, failure. The final mechanical strength of porous materials depends on the size, location and volume of these pores (Hardin & Beckermann, 2013). Low values of elastic modulus were also found by other authors for different materials produced by PM. Kuffner *et al.* (2018) investigated the reuse of metallic scraps of AISI 52100 tool steel, and the elastic modulus obtained for the sintered material were of 1.8 GPa (without addition of alumina in the milling process) and 2.5 GPa (with addition of 3% of alumina). In another study, carried out by Faria *et al.* (2018), in which they reused 316L stainless steel, the elastic modulus found was also low, corresponding to approximately 3% of the value of the material as casted. They verified the relationship between porosity and elastic modulus, and concluded that the samples with the highest pore volume were those with the lowest elastic modulus. These low values demonstrate that the high presence of porosity affects negatively the mechanical properties of any material produced by PM.

Table 7 – Elastic modulus of the sintered UNS S31803 duplex stainless steel with 3% of VC for conditions 1 and 3.

| Sample Condition 1 | Elastic modulus (GPa) | Sample Condition 3 | Elastic modulus (GPa) |
|---|---|---|---|
| 1 | 1.02 | 1 | 1.23 |
| 2 | 1.01 | 2 | 1.29 |
| 3 | 0.92 | 3 | 1.34 |
| 4 | 0.98 | 4 | 1.35 |
| 5 | 0.99 | 5 | 1.39 |
| Mean | 0.98 | Mean | 1.32 |
| Standard Deviation | 0.03 | Standard Deviation | 0.05 |

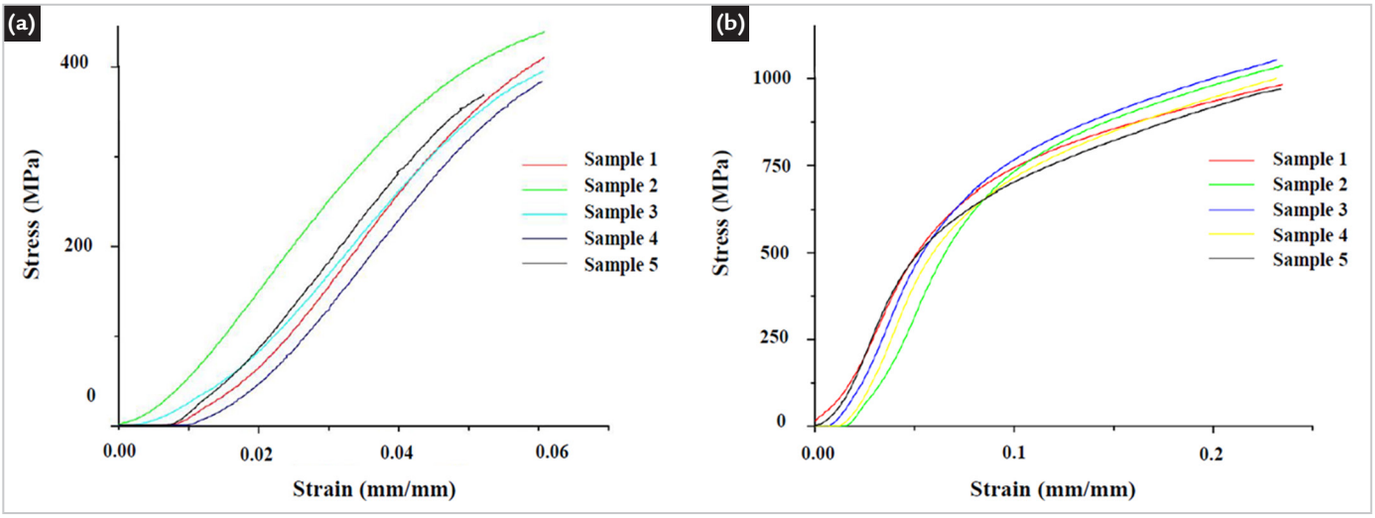


Figure 7 – Stress-strain curves of the sintered UNS S31803 duplex stainless steel with 3% of VC for conditions (a) 1 and (b) 3 (Table 3).

### 3.5 Hardness test

The results obtained in the hardness test are shown in Table 8. Six different points of each sample were evaluated, being then determined the standard deviation for all conditions.

Table 8 – Average hardness for all conditions of sintered UNS S31803 duplex stainless steel with 3% of VC.

| Condition | Rockwell Hardness (HRB) | Standard deviation |
|---|---|---|
| 1 | 70 | 2.0 |
| 2 | 72 | 3.3 |
| 3 | 86 | 2.3 |

It was observed that condition 3 presented a hardness substantially higher than the other conditions. Condition 1 showed an 18% higher hardness than condition 3, while condition 2, presented a 16% higher hardness, as a result of the advanced sintering stage. In addition, conditions 1 and 2 obtained similar hardness values, with

a small difference of 2.4% between them. When compared to the hardness found in literature for this steel of 96 HRB (Kwok *et al*., 1998), the results presented in Table 8 are lower, but very close. Conditions 1 presented 73% of this value, condition 2 presented 75% and condition 3, 90%. The best hardness values obtained by the samples subjected to higher compaction loads and sintering temperatures and times are a consequence of the lower porosity reached by them, which consequently implies in greater deformation resistance.

## 4. Conclusions

After the study to obtain a new metallic matrix composite from the recycling of UNS S31803 duplex stainless steel by powder metallurgy, it was possible to conclude that:

• The high energy ball milling (HEBM) process was an effective route to produce powders of UNS S31803 duplex stainless steel from its scraps, with the addition of vanadium carbide, obtaining a high fraction of micrometric particles, ranging from 7 to 209 μm and average size 42 μm.

• After HEBM, it was observed in the diffractogram the peaks enlargement and intensity decrease (amorphization), due to severe plastic deformation generated by the process, which causes deformation of the material crystalline lattice.

• The increase in compaction loads and sintering times and temperatures were fundamental to reduce the fraction of porosity of the material and, consequently, being responsible for the increase in the mechanical properties of the material. Condition 3 with the most severe parameters of pressing and sintering obtained better microstructural, physical and mechanical results.

• It was possible to prove the effectiveness of the powder metallurgy route (high energy ball milling, compacting and sintering) to produce a solid material from the UNS S31803 duplex stainless steel scraps, with the use of vanadium carbide. Although these components do not present the same mechanical strength than those produced from the casted material, they can be in the future tested under other parameters, such as wear resistance, to be used in other applications that demand lower mechanical strength.

## Acknowledgments

The authors would like to thank the CAPES for financial support. Also, the company Aperam South America for providing the UNS S31803 duplex stainless steel.

## References

AGUIAR, D. J. M. ***Processamento do aço inoxidável superduplex UNS S32520 por moagem de alta energia***. 2008. 99 f. Dissertação (Mestrado em Engenharia e Ciência de Materiais) - Universidade Estadual de Ponta Grossa, Ponta Grossa, 2008.

AMERICAN SOCIETY FOR TESTING AND MATERIALS. ***ASTM E09-19:*** Standard test methods of compression testing of metallic materials at room temperature. West Conshohocken, PA: ASTM International, 2019.

BARBEDO, E. L.; GONÇALVES, P. H.; LAMOGLIA, M. S.; PONTES, A. M. P.; KUFFNER, B. H. B., GOMES, G. F., SILVA, G. Analysis of milling efficiency of the Vanadis® 8 tool steel with additions of vanadium and molybdenum carbides. ***Materials Research***, v. 24, n. 5, p. 1-13, 2021.

DANNINGER, H.; CALDERON, R. O.; GIERL-MAYER, C. Powder metallurgy and sintered materials. *In*: ULLMANN'S Encyclopedia of Industrial Chemistry. Weinheim: Wiley-VCH, 2017.

DAVIS, J. R. (ed.). ***Stainless steels***. Ohio: ASM International, 1994. 576p. (ASM Specialty Handbook).

DIAS, A. N. O.; RODRIGUES, G.; MENDONÇA, C. S. P.; SILVA, G. Analysis of the densification of a composite obtained by sintering process of aluminum bronze powders with different carbides. ***REM - International Engineering Journal***, v. 72, n. 3, p. 461-467, 2019.

DZEPINA, B.; BALINT, D.; DINI, D. A phase field model of pressure-assisted sintering. ***Journal of the European Ceramic Society***, v. 39, n. 2-3, p. 173-182, 2019.

FARIA, M. H. A.; DIAS, A. N. O.; OLIVEIRA, L. A.; MENDONÇA, C. S. P.; KUFFNER, B. H. B.; SACHS, D.; SILVA, G. Microstructural and mechanical analysis of 316L SS/β-TCP composites produced though the powder metallurgy route. ***REM - International Engineering Journal***, v. 71, n. 4, p. 605-611, 2018.

GARCIA, C.; MARTIN, F.; BLANCO, Y. Effect of sintering cooling rate on corrosion resistance of powder metallurgy austenitic, ferritic and duplex stainless steels sintered in nitrogen. ***Corrosion science***, v. 61, p. 45-52, 2012.

GERMAN, R. M. ***Powder metallurgy and particulate materials processing: the processes, materials, products, properties and applications***. Princeton, New Jersey: Metal Powder Industries Federation, 2005. 528 p.

GUBERNAT, A. Z. L.; ZYCH, L. The isothermal sintering of the single-phase non-stoichiometric niobium carbide (NbC1-x) and tantalum carbide (TaC1-x). ***Journal of the European Ceramic Society***, v. 34, n. 12, p. 2885-2894, 2014.

GUNN, R. N. (ed.). ***Duplex stainless steels***: microstructure, properties and applications. [*S. l.*]: Woodhead Publishing, 1997. 204p. (Woodhead Publishing Series in Metals and Surface Engineering).

HARDIN, R. A.; BECKERMANN, C. Effect of Porosity on Deformation, Damage, and Fracture of Cast Steel. ***Metallurgical and Materials Transactions A***, v. 44, p. 5316-5332, 2013.

HUANG, K. T.; CHANG, S. H.; LEE, K. Y.; WU, M. W. Microstructural characteristics and properties of adding

vanadium carbide powders to Vanadis 4 tool steel through vacuum sintering and heat treatments. ***Materials Transactions***, v. 59, n. 10, p. 1596-1602, 2018.

INTERNATIONAL ORGANIZATION FOR STANDARDIZATION. ***ISO 4498***: Sintered metal materials, excluding hardmetals - Determination of apparent hardness and microhardness. Geneva, Switzerland: ISO, 2005.

KUFFNER, B. H. B.; SILVA, G.; RODRIGUES, C. A.; RODRIGUES, G. Study of the AISI 52100 steel reuse through the powder metallurgy route using high energy ball milling. ***Materials Research***, v. 21, n. 1, p. 1-10, 2018.

KWOK, C. T.; MAN, H. C.; CHENG, F. T. Cavitation erosion of duplex and super duplex stainless steels. ***Scripta Materialia***, v. 39, n. 9, p. 1229-1236, 1998.

MENDONÇA, C.; OLIVEIRA, A.; SACHS, D.; CAPELLATO, P.; RIBEIRO, V.; JUNQUEIRA, M.; MELO, M.; SILVA, G. A new method to recycle stainless–steel duplex UNS S31803 s. ***Metals***, v. 8, n. 7, p. 1-13, 2018.

OZOLA, Z. U.; VESERE, R.; KALNINS, S. N.; BLUMBERGA, D. Paper waste recycling. Circular economy aspects. ***Environmental and Climate Technologies***, v. 23, p. 260-273, 2019.

REUTER, M. A.; SCHAIK, A. V.; GUTZMER, J.; BARTIE, N.; ABADÍAS-LLAMAS, A. Challenges of the circular economy: a material, metallurgical, and product design perspective. ***Annual Review of Materials Research***, v. 49, p. 253-274, 2019.

SHASHANKA, R. D. C. Phase transformation and microstructure study of nano-structured austenitic and ferritic stainless steel powders prepared by planetary milling. ***Powder Technology***, v. 259, p. 125-136, 2014.

SURYANARAYANA C. Mechanical alloying and milling. ***Progress in Materials Science***, v. 46, n. 1-2, p. 1-184, 2001.

TAŃSKI, T.; BRYTAN, Z.; LABISZ, K. Fatigue behavior of sintered duplex stainless steel. ***Procedia Engineering***, v. 74, p. 421-428, 2014.

TOTTEN, G. E. ***Steel heat treatment handbook***. 2nd. ed. [*S. l.*]: CRC Press, 2006. 1576p.

TRUEMAN, A. R.; SCHWEINSBERG, D. P.; HOPE, G. A. A study of the effect of cobalt additions on the corrosion of tungsten carbide/carbon steel metal matrix composites. ***Corrosion Science***, v. 41, n. 7, p. 1377-1389, 1999.

YONEKUBO, A. E.; MOINHOS, C.; AGUIAR, D. J. M.; CAPOCCHI, J. D. T.; CINTHO, O. M. A morphological evaluation of a duplex stainless steel processed by high energy ball mill. *In*: INTERNATIONAL LATIN AMERICAN CONFERENCE ON POWDER TECHNOLOGY, 7., 2009, Atibaia, São Paulo. ***Proceedings*** [**...**]. [*S. l.*: *s. n.*], 2009. v. 1, p. 103-108.

Received: 27 September 2021 - Accepted: 14 March 2022.